

Clusters of Nanoscale Liposomes Modulate the Release of Encapsulated Species and Mimic the Compartmentalization Intrinsic in Cell Structures

Igor Kevin Mkam Tsengam,[†] Marzhana Omarova,[†] Lauren Shepherd,[†] Nicholas Sandoval,[†] Jibao He,[‡] Elizabeth Kelley,[§] and Vijay John^{*,†}

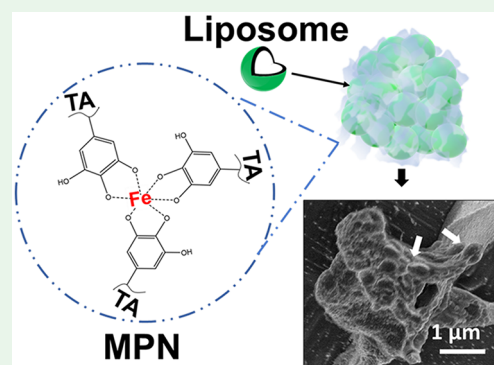
[†]Department of Chemical & Biomolecular Engineering and [‡]Coordinated Instrumentation Facility, Tulane University, 6823 St. Charles Avenue, New Orleans, Louisiana 70118, United States

[§]Center for Neutron Research, National Institute of Standards and Technology, Gaithersburg, Maryland 20899, United States

Supporting Information

ABSTRACT: We report the ability to place a high concentration of liposomes in a confined volume as a multicompartment cluster that mimics biological cells and allows for the modulation of release of encapsulated species. The formation of these coated multicompartmental structures is achieved by first binding liposomes into clusters before encapsulating them within a two-dimensional metal–organic framework composed of tannic acid coordinated with a metal ion. The essential feature is a molecularly thin skin over a system of clustered liposomes in a pouch. The structural features of these pouches are revealed by small-angle scattering and electron microscopy. Through cryogenic electron microscopy, clusters with intact liposomes are observed that appear to be encapsulated within a pouch. Small-angle X-ray scattering shows the emergence of a relatively weak Bragg peak at $q = 0.125 \text{ \AA}^{-1}$, possibly indicating the attachment of the bilayers of adjacent liposomes. The metal–phenolic network (MPN) forms a nanosized conformal coating around liposome clusters, resulting in the reduced release rate of the encapsulated rhodamine B dye. We further show the possibility of communication between the adjacent nanocompartments in the cluster by demonstrating enhanced energy transfer using fluorescence resonance energy transfer (FRET) experiments where the lipophilic donor dye 3,3'-dioctadecyloxycarbocyanine perchlorate (DiO) incorporated within one liposomal compartment transfers energy upon excitation to the lipophilic acceptor dye 1,1'-dioctadecyl-3,3,3',3'-tetramethylindocarbocyanine perchlorate (DiI) in a neighboring liposomal compartment due to their close proximity within the multicompartmental cluster. These observations have significance in adapting these multicompartmental structures that mimic biological cells for cascade reactions and as new depot drug delivery systems.

KEYWORDS: liposomes, metal–phenolic network, drug delivery, cell mimics, FRET



INTRODUCTION

Liposomes are artificial vesicles composed of a phospholipid bilayer with an aqueous core. They are of significant interest in drug delivery technologies due to their drug encapsulation capability and their ability to be taken by cells.^{1–5} The structural similarities between the lipid bilayers of liposomes and cell membranes have led to their use as cell membrane mimics.^{6–8} Cellular features such as the formation of multicompartmental systems have advanced the use of lipid-based vesicles in cell mimetics,^{9,10} and such systems may provide simplified experimental models to replicate and understand biological phenomena in controlled systems.¹¹ The development of structures with close resemblance to cells has been extended to the development of drug delivery systems^{12,13} and complex artificial multicompartment micro-reactors due to their ability to provide separation and protection of compounds within their internal compart-

ments.^{14,15} The potential to encapsulate a drug combination within lipid structures to be delivered simultaneously could have significant technical implications in combinatorial drug delivery.¹⁶

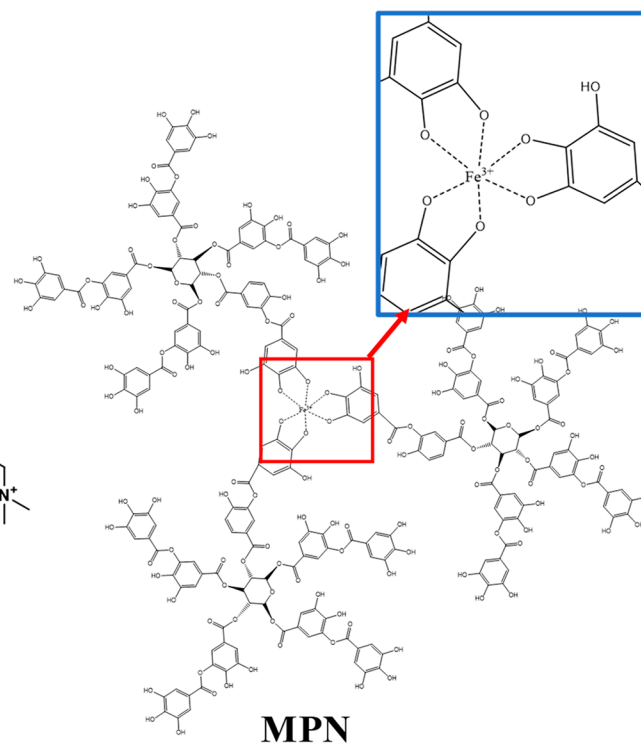
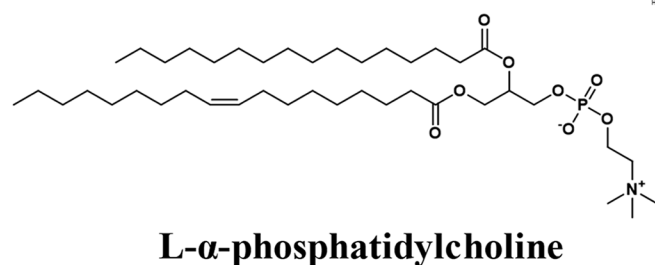
The formation of multicompartmental clusters has been demonstrated through methods such as encapsulation of small vesicles in the interior of giant vesicles,¹⁷ microfluidics,¹⁸ double-emulsion,¹⁹ and emulsion centrifugation.²⁰ While all such methods are extremely interesting in the development of new drug delivery systems, they may suffer from complexities in preparation and potentially damaging processing conditions such as the use of high shear rates. In this paper we show a simple way to bind liposomes into clusters and then generate a

Received: August 29, 2019

Accepted: October 23, 2019

Published: October 23, 2019

(a)



(b)

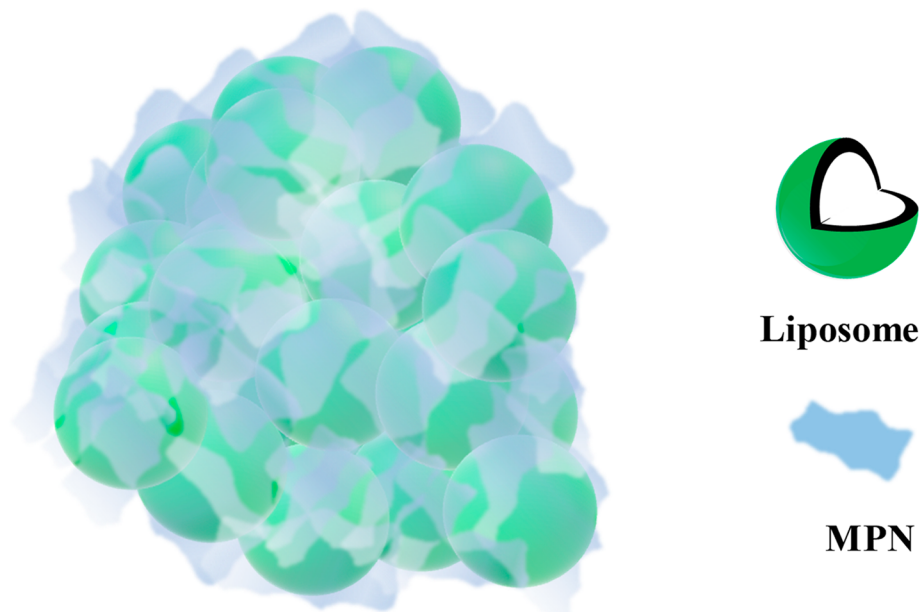


Figure 1. (a) Structures of L- α -phosphatidylcholine and metal–phenolic networks (MPN). Hydroxyl groups in tannic acid react with the Fe³⁺ ion to form MPN. (b) Schematic illustration of an MPN-coated liposome pouch.

thin coating over and throughout the cluster by encapsulating such vesicles within a two-dimensional metal–organic framework that acts as a skin around the vesicles. The system is assembled by coating glued vesicular compartments with supramolecular network structures composed of metal ions coordinated to a phenolic ligand, known as metal–phenolic networks (MPN). MPN are benign two-dimensional metal–organic frameworks pioneered by Ejima et al.²¹ They are composed of a natural occurring polyphenol such as tannic acid (TA), coordinated with a metal ion (Fe³⁺) (Figure 1a). Because of the high biocompatibility of the components constituting MPN and the ease with which they are assembled,

they have been used as coating for a number of biological applications. Thus, MPN have been used as cytoprotective coating for mammalian cells,²² bacteria,²³ and yeast.²⁴ In recent remarkable findings, Kumar and co-workers have demonstrated the coating of individual exosomes with a tannic acid–iron(III) chloride film as a cytoprotective film against external aggressors such as UV-C irradiation and heat.²⁵

In this paper, we explore the concept of easily fabricating a nanoscale system where liposomes are first placed in a confined volume by gluing them together without disruption of the vesicles and are then subsequently covered with a skin of MPN. The glue is simply the polyphenolic species where we

exploit the fact that polyphenolics exhibit properties of adhesion to surfaces in water expressed most remarkably by the catechol-based proteins responsible for the underwater adhesive properties of mollusks.²⁶ Early recognition that polyphenolics can bridge lipid bilayers has been shown in elegant studies by Simon and co-workers.^{27,28} More recently, the formation of bridges between lipid bilayers containing small phenolic lipids and flavonoids modulated by metal atoms has been demonstrated.^{29,30} We exploit these concepts to place a high concentration of vesicles in a confined volume as a coated multicompartamental container which can then be used in depot-based drug delivery applications. These drug depots could offer reduced dosing frequency due to the localized availability of large amounts of drugs. Additionally, the proximity of the individual nanocompartments within the liposome pouches may allow the feature of enhanced communication between liposomal compartments.

Thus, by utilizing the intrinsic adhesive properties of tannic acid as the model polyphenol, we bind liposomes into clusters before adding the metal ion to form MPN on the surface of these clusters, resulting in coated multicompartamental liposome pouches. We show unique features such as the ability of MPN to conform onto the surface of aggregated vesicles in coated pouch-like structures with the ability to modulate the release of encapsulated species from the internal compartments. We also demonstrate the possibility of communication between adjacent nanoscale liposomal compartments through a simple fluorescence resonance energy transfer (FRET) experiment with donor and acceptor lipophilic dyes incorporated into separate liposomal compartments.

The objectives of this study are to (1) form MPN-coated multicompartamental lipid-based systems with emphasis on defining their structural features and demonstrating their ability to modulate the release of encapsulated cargo within their nanocompartments and (2) facilitate intercompartment communication through confinement. Using small-angle X-ray scattering (SAXS), small-angle neutron scattering (SANS), and cryogenic transmission electron microscopy (cryo-TEM), we obtain a nanoscale understanding of the structural features of such MPN-coated liposomal pouches.

MATERIALS AND METHODS

Materials. *L*- α -Phosphatidylcholine (95%) extracted from soybeans was purchased from Avanti Polar Lipids. Tannic acid, iron(III) chloride hexahydrate ($\text{FeCl}_3 \cdot 6\text{H}_2\text{O}$), 3,3'-dioctadecyloxycarbocyanine perchlorate (DiO), 1,1'-dioctadecyl-3,3,3',3'-tetramethylindocarbocyanine perchlorate (DiI), hydrochloric acid (HCl, 37%), fluorescein isothiocyanate-dextran (FITC-dextran, M_w 3–5 kDa), and rhodamine B were purchased from Sigma-Aldrich. Phosphate buffered saline was purchased from Fisher Scientific. Deuterium oxide (D_2O , 99.9%) was obtained from Cambridge Isotopes Laboratory. Deionized (DI) water generated by an ELGA reverse osmosis water purification system (MEDICA 15BP) with a resistance of 18.2 $\text{M}\Omega\text{-cm}$ was used in all experiments.

Liposome Preparation. *L*- α -Phosphatidylcholine (PC) liposomes were prepared by using the thin film hydration method.³¹ PC (0.1 g) was first dissolved in a round-bottomed flask by 15 mL of a mixed solution of chloroform and methanol at a volume ratio of 2:1. The solvent was then evaporated by using a rotary evaporator (Buchi R-205) at room temperature under 100 mbar for 3 h to form a thin lipid film. The pressure was further reduced to 6 mbar for 30 min to remove the residual solvent. The obtained thin lipid film was hydrated with PBS buffer at 50 °C for 30 min. The aqueous suspension was transferred to a syringe and extruded 21 times through a 100 or 800 nm polycarbonate membrane.

MPN-Coated Liposome Pouches Preparation. Metal-phenolic network (MPN)-coated liposome pouches were prepared by sequentially adding 10 μL of tannic acid stock solution (40 mg mL^{-1} in DI water) and 10 μL of iron(III) chloride stock solution (10 mg mL^{-1} in DI water) to 1 mL of 0.25% liposome solution in PBS buffer (pH 7.4) with 30 s of vortex mixing between the additions (6.25:1, lipid:tannic acid weight ratio and a 4:1 TA: Fe^{3+} weight ratio). The resulting suspension was vortex mixed for 30 s.

Fluorescence Microscopy. Fluorescence microscopy was used to visualize the MPN-coated liposome pouches. FITC-dextran was encapsulated within liposomes. The following procedure was used to encapsulate FITC-dextran within liposomes. PC was first dissolved in a round-bottomed flask by a mixed solution of chloroform and methanol at a volume ratio of 2:1. The lipid film was hydrated by using 1 mg/mL of FITC-dextran solution at 50 °C for 30 min. The aqueous suspension was transferred to a syringe and extruded 21 times through an 800 nm polycarbonate membrane. Unencapsulated FITC-dextran was removed by dialyzing through a dialysis bag (M_w cutoff: 12–14 kDa) against a 100:1 PBS bath volume at 25 °C for 1 h. MPN coating was applied to the dye-encapsulated liposomes by sequentially adding tannic acid and iron(III) chloride to the dye-encapsulated liposomes at a 6.25:1 lipid:tannic acid weight ratio and a 4:1 tannic acid:iron(III) chloride weight ratio. Thirty seconds of vortex mixing was applied after the addition of tannic acid and iron(III) chloride. One hundred microliters of FITC-dextran-loaded liposomes or MPN-coated liposome pouches was placed in the microscope stage and imaged by using confocal microscopy (Leica SP2 AOBS 2004) with an oil immersion objective.

Cryo-Scanning Electron Microscopy (Cryo-SEM). The surface morphologies of the liposomes and the MPN-coated liposome pouches were imaged by cryogenic scanning electron microscopy (cryo-SEM). Prior to imaging, the samples were frozen. The following procedure was used to freeze the samples. Briefly, the samples were transferred into rivets mounted onto the cryo-SEM sample holder. The samples were frozen by submersion into slushed liquid nitrogen to freeze the sample. This was followed by fracturing at -130 °C using a flat-edge cold knife and sublimation of the solvent at -95 °C for 10 min to remove surface vitrified water. The temperature was lowered back to -130 °C, and the sample was then sputtered with a gold-palladium composite at 10 mA for 88 s followed by 44 s before imaging.

Cryo-Transmission Electron Microscopy (Cryo-TEM). Cryo-TEM imaging was done on a FEI G2 F30 Tecnai TEM operated at 200 kV to obtain high-resolution imaging of liposomes prepared by extrusion 21 times through a 100 nm polycarbonate membrane and liposomes within the cluster. The sample was prepared by using a FEI Vitrobot. Five microliters of the sample was applied to a 200-mesh lacey carbon grid (Electron Microscopy Sciences). Excess liquid was blotted by filter paper attached to the arms of the Vitrobot for 2 s to form a thin film. The sample was then vitrified by plunging into liquid ethane followed by liquid nitrogen. The vitrified sample was finally transferred onto a single-tilt cryo-specimen holder for imaging. The cryo-holder was maintained below 170 °C to prevent sublimation of vitreous water.

Zeta-Potential, X-ray Photoelectron Spectroscopy (XPS), and X-ray Diffraction (XRD). The zeta-potential measurements were conducted using a Nanobrook ZetaPALS (Brookhaven Instruments). XPS measurements were conducted on a VG Scientific MKII system using an Al $K\alpha$ anode as excitation source ($h\nu = 1486.6$ eV). The pressure in the chamber during analysis was $<2 \times 10^{-8}$ mbar. The XRD measurement was conducted on a Siemens D 500 using Cu $K\alpha$ radiation at a wavelength of 1.54 Å.

Small-Angle Scattering. Small-angle neutron scattering (SANS) measurements were made on the 30 m SANS Instrument at the National Institute of Standards and Technology (NIST) Center for Neutron Research (NCNR) in Gaithersburg, MD. The samples were prepared with pure deuterium oxide to generate enough scattering contrast. All measurements were conducted at 25 °C. The raw data were corrected for the empty cell and background by using the macros provided by the NCNR.³² The data are presented as absolute

intensity versus the wave vector $q = 4\pi \sin(\theta/2)/\lambda$, where λ is the wavelength of incident neutrons and θ is the scattering angle.

Small-angle X-ray scattering (SAXS) experiments were performed at the Advance Photon Source on beamline 12-BM. All measurements were conducted with the 12 keV beam. All measurements were conducted at 25 °C. The samples were loaded in 1.5 mm quartz capillaries and placed on a sample holder at a sample-to-detector distance of 2 m. The data are presented as absolute intensity versus the wave vector $q = 4\pi \sin(\theta/2)/\lambda$, where λ is the wavelength and θ is the scattering angle. The reduction of SAXS data and background subtraction were performed by using Irena SAS macros on IGOR pro software.³³

Fluorescence Resonance Energy Transfer (FRET). FRET experiments were conducted to demonstrate communication between adjacent compartments. Two liposomal solutions with lipophilic dyes, 3,3'-dioctadecyloxycarbocyanine perchlorate (DiO) and 1,1'-dioctadecyl-3,3,3',3'-tetramethylindocarbocyanine perchlorate (DiI), incorporated within their bilayers were prepared. DiO and DiI are highly lipophilic and have a very low solubility in water.³⁴ Briefly, PC was first dissolved in a round-bottomed flask containing a mixture of chloroform and methanol at a volume ratio of 2:1. The lipophilic dyes DiI or DiO were added at 0.5 wt % of PC to the mixture of PC in chloroform and methanol. The solvent was then evaporated by using a rotary evaporator (Buchi R-205) at 25 °C. The obtained thin lipid film was hydrated with PBS for 30 min at 50 °C to obtain a 0.5% overall lipid weight percent. The aqueous suspension was transferred to a syringe and extruded 21 times through an 800 nm polycarbonate membrane. Equal volumes of DiI and DiO incorporated liposomes were mixed with increasing amounts of tannic acid vortex mixed for 30 s. The emission spectra of the liposome–tannic acid mixtures were obtained by using a BioTek Synergy H1 microplate reader (Winooski, VT) excited at 458 nm.

Dye Encapsulation and Release Experiment. The following procedure was used to encapsulate rhodamine B, a hydrophilic dye which can permeate through liposomes. Briefly, 0.05 mg/mL of rhodamine B solution was used to hydrate PC lipid film at 50 °C for 30 min. The mixture was extruded through a 100 nm filter size polycarbonate membrane to obtain dye encapsulated liposomes. Unencapsulated rhodamine B was removed by rapidly dialyzing through a dialysis bag (M_w cutoff: 12–14 kDa) against a 100:1 PBS bath volume at 25 °C until negligible rhodamine B was detected in the external solution by observing the fluorescence emission at 627 nm after excitation at 553 nm. The amount of encapsulated dye was evaluated by measuring the sample's total fluorescence as determined after micellization by using Triton X. An EnSpire Multimode Plate Reader on excitation and emission wavelengths of 627 and 553 nm, respectively, was used for fluorescence measurements. To dissolve the lipid for dye encapsulation measurements, 10% (v/v) of Triton X in PBS was added to the dye-encapsulated liposome solution at a liposome solution to Triton X solution volume ratio of 1:1. The amount of dye encapsulated was determined by using the calibration curve for rhodamine B in aqueous Triton X solutions.

The rhodamine B release profiles from dye-loaded liposomes and MPN-coated liposome pouches were determined by the dialysis method. The release experiments were conducted by dialyzing 2 mL of the dye-loaded liposome against 20 mL receptor medium at 37 °C. Two milliliters of rhodamine B-loaded liposomes was encapsulated within MPN by sequentially adding tannic acid and iron(III) chloride at a 6.25:1 lipid:tannic acid weight ratio and a 4:1 tannic acid:iron(III) chloride weight ratio and placed in a dialysis bag for release experiments. Rhodamine B release at acidic pH was achieved by dropwise addition of 0.2 mol/L HCl to a pH of 4 to liposomes and MPN-coated liposome pouches and placed in dialysis bags. At precise time intervals, 1 mL of receptor medium was taken out for analysis, and fresh receptor medium was replenished. The concentration of the released rhodamine B was measured by measuring the fluorescence intensity of 100 μ L of the extracted sample by using an EnSpire Multimode Plate Reader at an excitation wavelength of 627 nm and an emission wavelength of 553 nm. All data reported are the mean value with standard deviation of three different experiments.

RESULTS AND DISCUSSION

Characterization of MPN-Coated Liposome Pouches. Imaging Studies. Formation of the MPN-coated liposome pouches was examined by using confocal microscopy, and morphological characteristics were studied through cryogenic scanning electron microscopy (cryo-SEM). Figure 2 illustrates

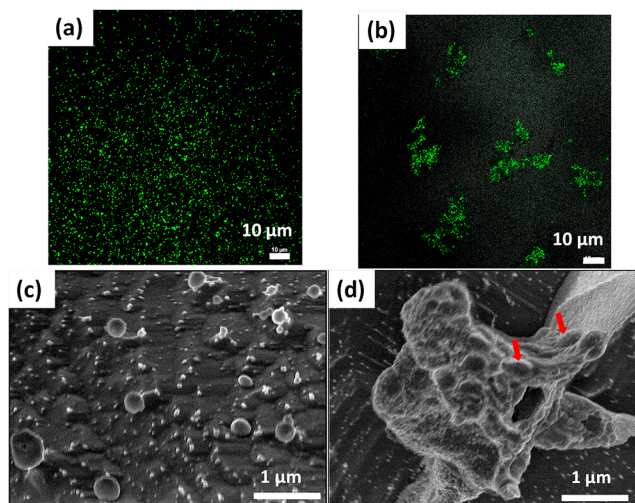


Figure 2. Imaging of liposomal pouches using confocal microscopy and cryo-SEM. (a) Confocal microscopy image of nonaggregated liposomes with encapsulated FITC–dextran and of (b) MPN-coated liposome pouches with liposomes containing the dye. The clustering of the fluorescence pattern indicates aggregated liposomes in a pouch. (c) Cryo-SEM of individual liposomes. (d) Cryo-SEM of an MPN-coated liposome pouch. Liposomes are mixed with tannic acid at a 6.25:1 lipid to tannic acid weight ratio and a 4:1 tannic acid to iron(III) chloride weight ratio to form the pouch.

clear differences between liposomes (Lip) and MPN-coated liposome pouches (MPNLip). As shown in Figure 2a, the native liposomes loaded with FITC–dextran appear as distinct fluorescent specks on the confocal micrograph, with the large fluorescent tag being stably encapsulated within the liposomes for extended periods.³⁵ Upon sequential addition of tannic acid and iron(III) chloride to liposomes at a 6.25:1 lipid to tannic acid weight ratio and 4:1 tannic acid to iron(III) chloride weight ratio, we observe the formation of fluorescent clusters that are easily greater than 10 μ m. The formation of these fluorescent clusters is an indication of liposome aggregation and encapsulation into the MPN pouches. However, the fluorescence analysis is insufficient to determine whether the liposomes retain their integrity, and we used cryo-SEM to image these systems at a much higher resolution. Native liposomes are nonaggregated and spherical (Figure 2c), and we clarify that the dots in the cryo-SEM are artifacts constituting small water crystals that remain after vitrification. On the other hand, in Figure 2b we clearly observe the presence of aggregated liposomes covered by a coating, after the sequential addition of tannic acid and iron(III) chloride. These coated aggregates are composed of intact liposomes as highlighted by arrows in Figure 2d showing the distinct outline of the liposomes. Cryo-SEM indicates that the MPN attached to the surfaces of the aggregated liposomes, resulting in the formation of MPN-coated liposome pouches. After encapsulation of the liposomes within the metal–phenolic networks, there is an increase in the negative potential (from -1 ± 2 to -8 ± 1

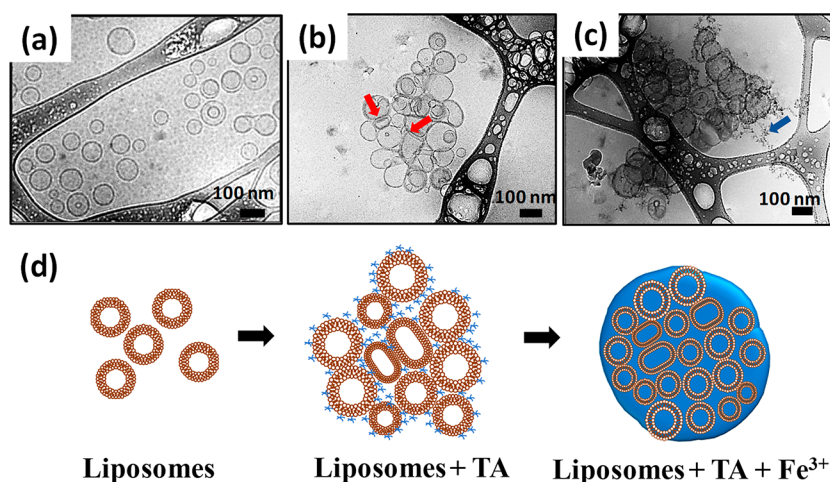


Figure 3. Cryo-TEM imaging showing transitions to liposome encapsulation in a pouch. (a) Cryo-TEM of individual liposomes. (b) Aggregate formed due to the addition of tannic acid to liposomes at a 6.25:1 lipid to tannic acid weight ratio. (c) MPN-coated liposome pouch formed after the addition of iron(III) chloride to a liposome–tannic acid mixture at a 4:1 tannic acid to iron(III) chloride weight ratio. The MPN coating is observed as a darkening of the TEM image, and the arrow points to wisps of MPN at the edges of a cluster. (d) Schematic illustration of the sequential formation of MPN-coated liposome pouches.

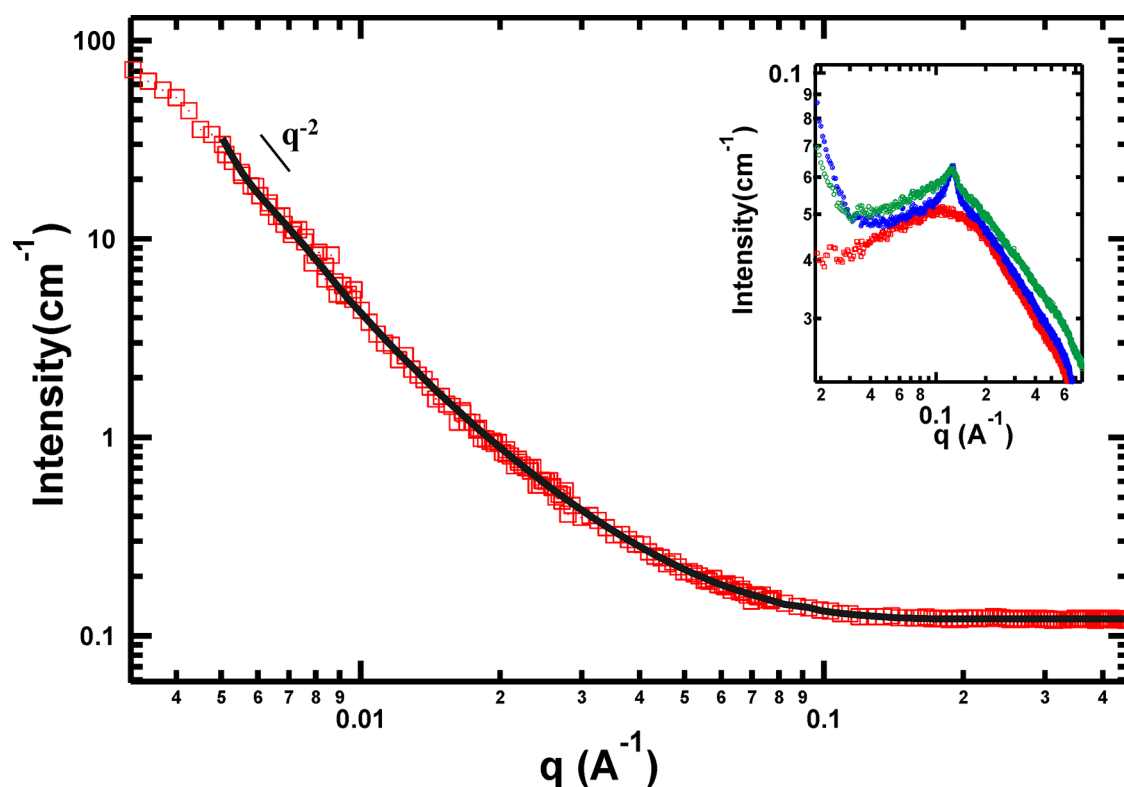


Figure 4. SANS profile of 0.25% liposomes. The black solid line shows best-fit results to the core–shell model. The inset shows SAXS profiles of 0.25% liposomes (red), liposomes mixed with tannic acid (blue), and liposomes mixed with tannic acid and iron(III) chloride (green). Liposomes were mixed with tannic acid at a 6.25:1 lipid to tannic acid weight ratio and a 4:1 tannic acid to iron(III) chloride weight ratio. The emergence of the Bragg peak suggests the occurrence of layered structures with uniform spacing.

mV), which we ascribe to the hydroxyl functional groups of the galloyl groups in the MPN structure.²¹ The energy dispersive X-ray (EDX) elemental mapping of the dried coated pouches confirms the presence of iron in their microstructures (Supporting Information S11). Additionally, the XPS spectra of MPN-coated liposome pouches show the emergence of the Fe 2p signal at 713 eV with a 2p peak split of 13 eV, indicating the presence of Fe³⁺ species in the MPN coating (Supporting

Information S12).³⁶ The liposome suspension has a bluish tinge upon addition of tannic acid and iron(III) chloride due to the formation of the MPN complex (Supporting Information S13).^{21,37}

The microstructures of tannic acid-induced aggregated liposomes (TALip) and MPN-coated liposome pouches (MPNLip) were also imaged by using cryo-TEM to obtain high-resolution imaging of intact liposomes within the cluster

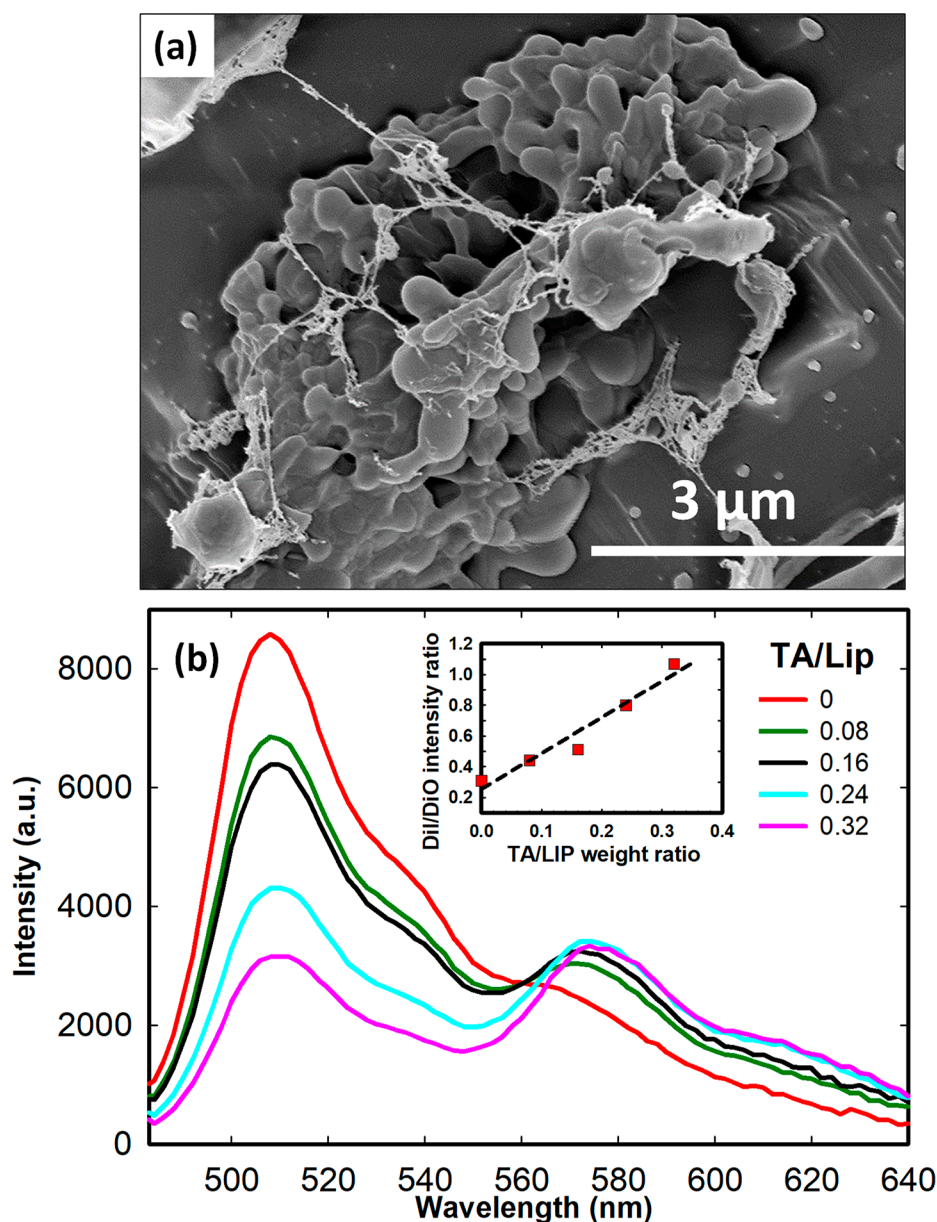


Figure 5. (a) Cryo-SEM of a liposome cluster formed through the addition of tannic acid to liposomes at a 6.25:1 lipid to tannic acid weight ratio. (b) Emission spectra of liposome–tannic acid mixtures (excitation wavelength 458 nm). Equal volumes of DiI and DiO incorporated liposomes were mixed with increasing amounts of tannic acid. The inset shows the correlation between the DiI/DiO peak intensity ratio and TA/Lip weight ratios.

(Figure 3). Figure 3a shows the distinct morphology of individual liposomes that are in the 100 nm size range. A few bilamellar liposomes and fused liposomes are observed, but generally the observed liposomes are distinct and separated from each other.

Figure 3b shows the result of introducing tannic acid at a 6.25:1 lipid to tannic acid weight ratio; it is clearly observed that the liposomes aggregate into clusters, and there is evidence of distortion of spherical morphology and flattening of bilayers at the contact planes between liposomes. Figure 3c shows a TEM image of a cluster after adding Fe^{3+} to form MPN through linkage of tannic acid moieties. The darker covering over the cluster indicates the MPN layer, and a few wisps of MPN are observed at the edges of the cluster. It is important to note that neither tannic acid addition nor the

formation of MPN grossly destroys the structural integrity of individual liposomes.

We note that liposome pouches can also be formed through a process where MPN are first synthesized and then directly added to liposomes to form pouches of liposomes in MPN. The X-ray diffraction (XRD) measurement of the metal phenolic networks shows no evidence of a crystalline material, and the diffraction pattern only shows a broad band, which is in agreement with the literature on XRD of metal–phenolic networks (Supporting Information S14).³⁸ EM imaging of a cluster formed by adding the synthesized MPN to liposomes is shown in the Supporting Information S15.

Small-Angle Scattering. SANS and SAXS experiments were conducted to obtain an understanding of the structural features of the MPN-coated liposome pouches. The scattering intensity, $I(q)$, is determined by the structure factor, $S(q)$,

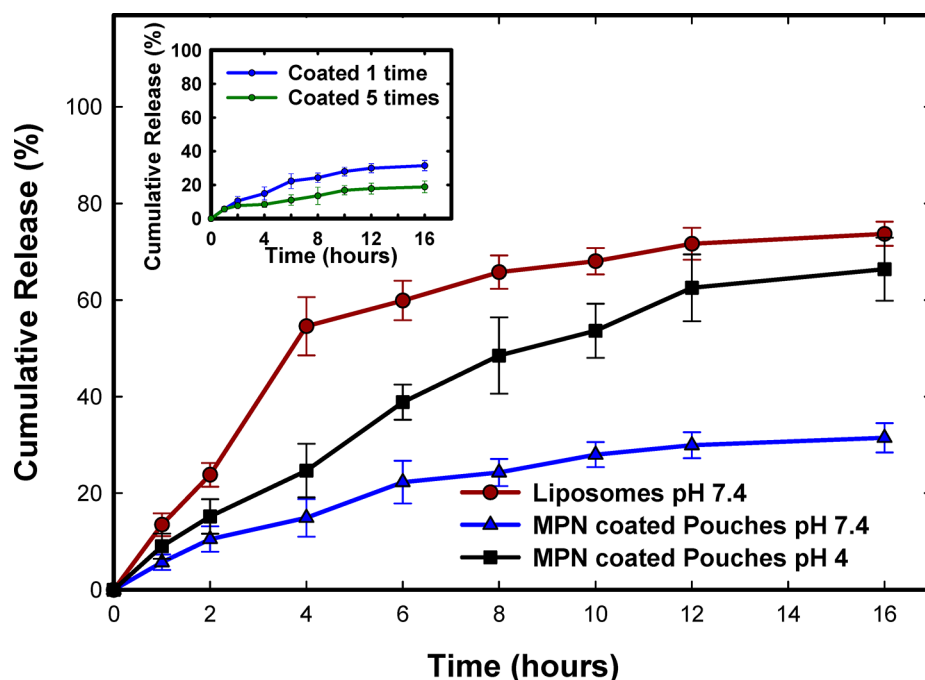


Figure 6. Time-dependent release of rhodamine B from liposomes and MPN-coated liposome pouches. The MPN coating around the pouches slows the release of rhodamine B from the internal compartments of the pouches. Disassembly of the MPN results in a faster release of rhodamine B. The inset shows the effect of multiple coatings on rhodamine B release.

and the form factor, $P(q)$. For a dilute dispersion of noninteracting vesicles, the intensity can be accounted for purely in terms of the form factor $P(q)$ ($S(q)$ close to 1).³⁹ The plot in Figure 4 shows the SANS scattering profile of a 0.25% liposome solution. For a detailed analysis of the form factor in this dilute system, the scattering data were fitted to the Coreshell model using SASView software.⁴⁰ This model provides the form factor $P(q)$ for a spherical particle with a core-shell structure⁴¹

$$P(q) = \frac{\text{scale}}{V} F^2(q) + \text{background} \quad (1)$$

with

$$F^2(q) = \frac{3}{V_s} \left[V_c (\rho_c - \rho_s) \frac{\sin(qr_c) - qr_c \cos(qr_c)}{(qr_c)^3} + V_s (\rho_s - \rho_{\text{solv}}) \frac{\sin(qr_s) - qr_s \cos(qr_s)}{(qr_s)^3} \right] \quad (2)$$

where V_s is the volume of the whole particle, V_c is the volume of the core, V_s is the volume of the whole core, r_s = radius + thickness is the radius of the particle, r_c is the radius of the core, ρ_c is the scattering length density of the core, ρ_s is the scattering length density of the shell, and ρ_{solv} is the scattering length density of the solvent.

The scattering profile of the liposome system indicates a q^{-2} dependence in the low q range, which is characteristic of noninteracting liposomes.^{42,43} The solid line shows the best fit of the scattering data. The fitting results show a liposome diameter of 99.0 nm with a polydispersity of 0.41 and a shell thickness (the lipid bilayer) of 3.30 nm. We have not shown the SANS data for the TALip and MPNLip because over the 1 h acquisition time for SANS these systems form large aggregates of liposomes that are not colloidally stable and

fall out of the neutron beam, making direct extraction of structural information difficult. We were able to obtain structural information for TALip and MPNLip from SAXS over the 1 min data acquisition time, which is sufficient for the experiment during which the liposomal clusters remain suspended in solution. The results shown in Figure 4 indicate the clear emergence of a Bragg peak at $q = 0.125 \text{ \AA}^{-1}$. The emergence of the Bragg peak possibly verifies the attachment of two bilayers perhaps mediated by TA, leading to the occurrence of layered structures with uniform spacing. The Bragg peak indicates a periodicity ($d = 2\pi/q$) of 5.0 nm between scattering planes (center-center distance between two bilayers). With a shell thickness of 3.3 nm from SANS, this indicates a gap of 1.7 nm between bilayers.

Compartmentalization Monitored by FRET. A key objective in encapsulating liposomes in pouches is to bring the vesicular compartments in close proximity to determine whether there is communication between them, an essential feature of compartments in a living cell. We do this by considering the possibility of enhanced energy transfer between vesicular compartments in the pouch as opposed to vesicles in solution, using fluorescence resonance energy transfer (FRET) experiments where a donor molecule in one compartment transfers energy upon excitation to an acceptor molecule in another compartment. For the FRET experiments, equal volumes of two liposomal solutions, one incorporating the lipophilic donor dye (DiO) and the other incorporating the lipophilic acceptor dye (DiI), were mixed, and the liposomes were aggregated simply by using tannic acid. The cryo-SEM of Figure 5a shows a tight aggregation of liposomes due to the addition of tannic acid at a lipid to tannic acid weight ratio of 6.25:1. As shown in Figure 5b, there is clear evidence of enhanced energy transfer upon tannic acid-induced vesicle aggregation through a reduction of the donor peak intensity and an increase in the acceptor peak intensity.⁴⁴

We note that we conducted the FRET experiments with just tannic acid to form liposomal clusters and that we did not further connect the tannic acid with Fe^{3+} to form MPN. This is due to the observation that the signal intensities are decreased significantly by the addition of the MPN coatings as shown in the Supporting Information SI6. To verify that this reduction in signal intensity is not due to quenching by Fe^{3+} , we measured the signal intensity of DiO-incorporated liposomes exposed to increasing amounts of Fe^{3+} metal ions. There is no significant change in the signal intensity with increase in the amount of Fe^{3+} ions as shown in the Supporting Information SI6 (Figure S6b). We therefore postulate that the reduction in signal intensity is due to the MPN blocking the entry of radiation into the interior of the pouches.

Figure 5b shows the results of the FRET experiments with the curve at TA/Lip of 0, indicating the control of nonclustered liposomes. In resonance energy transfer (RET), the efficiency of energy transfer $E = R_0^6/[R_0^6 + r^6]$, where R_0 is the characteristic Förster transfer radius for a specific dye pair and r is the distance between the donor and acceptor. The DiO–DiI FRET pair has a Förster transfer radius of 4.2 nm,³⁴ and when the distance between the pair is the same as the Förster transfer radius ($r = R_0$), the efficiency of energy transfer is 50%. The efficiency is also expressed by $E = 1 - F/F_0$, where F and F_0 are the donor luminescence intensities in the absence and in the presence of the acceptor (quencher).³⁴ Figure 5b clearly indicates energy transfer in the cluster with the signal intensities from the acceptor increasing with the level of TA. Efficiencies of 50% are obtained at TA/Lip ratios of 0.24 and higher, and with the assumption that in the absence of TA the large separation distance leads to negligible energy transfer, we can infer that there are significant donor–acceptor pairs separated by distances below the Förster transfer radius at TA/Lip ratios of 0.24 or greater. Because the bilayer thickness obtained from SANS is 3.3 nm and the Bragg peak indicates a d spacing of 5.0 nm, the gap between adjacent bilayers is 1.7 nm. Thus, immobilization of the donor and acceptor in adjacent bilayers brings the separation distance to values that are of the order of the Förster transfer radius with increasing TA levels leading to more FRET pairs being within the separation distance for efficient energy transfer. The inset to Figure 5b shows an approximate linear correlation of the DiI to DiO peak ratio with TA addition, which we attribute to increased clustering. We note that at tannic acid levels beyond a TA/Lip weight ratio of about 0.4 large aggregates are formed that precipitate out from solution.

Release of Encapsulated Rhodamine B from Liposome Pouches. Figure 6 shows characteristics of the release of Rhodamine B from liposomes (Lip) and MPN-coated liposomes (MPNLip). The control sample of nonclustered liposomes (Lip) shows release characteristics that are invariant to changes in pH level as described in the Supporting Information SI7. The MPNLip system shows significantly reduced release rate of the model compound which we attribute to the coating. We note that MPN do not constitute a complete seal to the release of rhodamine B, and the earlier work by Ejima et al.²¹ has shown that capsules of MPN can take fluorescent dyes from the bulk solution. Multiple coatings of MPN decrease the release rate from the liposomal pouch even further as shown in the inset to Figure 6. Disassembly of MPN was achieved by adjusting the pH of the MPN-coated liposome pouches to 4, and the release curve of the disassembled MPN-coated pouches shows an increase in

release rates compared to release from the pouches maintained at a pH of 7.4. The release rates observed are lower than those of the pristine liposome system (Lip). We attribute this observation to the TA coating that remains on the liposomes. We imaged the disassembled system at pH 4 (Supporting Information SI8) and verified the structural integrity of liposomes after removal of the MPN coating and a continued clustering due to the presence of TA. The images resemble those of liposomes simply tied together with TA as seen in Figure 5a.

CONCLUSIONS

In this study, we have developed a coated multicompartmental cluster based on binding liposomes using polyphenols and subsequently forming metal–polyphenol networks (MPN) to generate essentially two-dimensional coatings akin to a skin on these clustered vesicles. The final system resembles a cluster of liposomes in a pouch with each liposome representing a nanoscale compartment in the pouch. These confined vesicular systems are shown to function as nanocontainers for the encapsulation and controlled release of model compounds from within their internal compartments. The intrinsic biocompatibility of the components of the MPN-coated liposome pouches and the fact that they can be rapidly assembled have significant technical implications in depot drug delivery. It is observed that the liposomes are remarkably intact within the pouches and that the release rate is controlled by the level of MPN used. Additionally, the MPN-coated liposome clusters can be applied as a novel injectable depot formulation for the localized delivery of chemotherapeutic drugs, where the pouches can be directly injected into accessible tumors without being easily cleared. The extracellular pH of solid tumors is slightly acidic⁴⁵ and will lead to a slow degradation of the MPN coating. Thus, tumor microenvironments can be targeted through low-pH triggered drug release from the MPN-coated liposome pouches. In earlier work from our laboratory, we have shown the synergy of high-intensity focused ultrasound (HIFU) with liposomal delivery of chemotherapeutics to tumors.⁴⁶ We hypothesize that with the high loading depots of chemotherapeutics injected into the tumor microenvironment it may be possible to increase the efficiency of HIFU even further, and these are objectives of our continuing research.

Furthermore, the compartmentalized structure of the MPN-coated liposome pouches simulates the multicompartmentalization in a biological cell, and these systems may serve to generate new concepts in cell mimetics. Through a simple FRET experiment we have shown improved energy transfer between molecules from one vesicle bilayer to a separate vesicle bilayer when the vesicles are brought into close confinement within the pouch. Thus, the proximity of compartments provides the possibility of communication between compartments. Our continuing research seeks to exploit the structural features of liposome pouches in realizing new applications in depot drug delivery, in the development of lipid-based compartmentalized microreactors, and in generating artificial mimics of cell function.

ASSOCIATED CONTENT

Supporting Information

The Supporting Information is available free of charge on the ACS Publications website at DOI: 10.1021/acsanm.9b01659.

Elemental analysis of an MPN-coated liposome pouch showing the presence and distribution of iron within the MPN-coated liposome pouch (SI1); XPS spectra of liposomes, MPN, and MPN-coated liposome pouches (SI2); photographs of a liposomal solution and a solution of MPN-coated liposome pouches (SI3); XRD spectra of metal-phenolic networks (SI4); cryo-TEM imaging of an MPN-coated liposome pouch formed through a process where MPN are first synthesized and then directly added to liposomes (SI5); emission spectra of liposome clusters and MPN-coated liposome clusters (excitation wavelength 458 nm), emission spectra of liposomes mixed with iron(III) chloride at different lipid:Fe³⁺ weight ratios (excitation wavelength 458 nm) (SI6); time-dependent release of rhodamine B from liposomes at pH 7.4 and liposomes at pH 4 (SI7); cryo-SEM of a disassembled MPN-coated liposome pouch (SI8) (PDF)

AUTHOR INFORMATION

Corresponding Author

*(V.T.J.) E-mail vj@tulane.edu.

ORCID

Igor Kevin Mkam Tsengam: 0000-0002-6587-0555

Lauren Shepherd: 0000-0001-6720-5439

Nicholas Sandoval: 0000-0002-1743-3975

Elizabeth Kelley: 0000-0002-6128-8517

Vijay John: 0000-0001-5426-7585

Notes

The authors declare no competing financial interest.

ACKNOWLEDGMENTS

Small-angle X-ray scattering performed at the Advanced Photon Source at Argonne National Laboratories was supported by the U.S. Department of Energy under EPSCoR Grant DE-SC0012432. Small-angle neutron scattering was done at the National Center for Neutron Research, National Institute for Science and Technology. We are also grateful for funding from the National Science Foundation Grant 1805608. We acknowledge assistance from Dr. Xiaodong Zhang in XPS analysis. We acknowledge Dr. Sungsik Lee (Advanced Photon Source, Argonne National Laboratory) for assistance with SAXS studies.

REFERENCES

- (1) Barenholz, Y. Doxil (R) - the First FDA-Approved Nano-Drug: Lessons Learned. *J. Controlled Release* **2012**, *160* (2), 117–134.
- (2) Meunier, F.; Prentice, H. G.; Ringden, O. Liposomal Amphotericin-B (Ambisome) - Safety Data from a Phase-II/III Clinical-Trial. *J. Antimicrob. Chemother.* **1991**, *28*, 83–91.
- (3) Park, J. W. Liposome-Based Drug Delivery in Breast Cancer Treatment. *Breast Cancer Res.* **2002**, *4* (3), 93–97.
- (4) Dhule, S. S.; Penfornis, P.; He, J. B.; Harris, M. R.; Terry, T.; John, V.; Pochampally, R. The Combined Effect of Encapsulating Curcumin and C6 Ceramide in Liposomal Nanoparticles against Osteosarcoma. *Mol. Pharmaceutics* **2014**, *11* (2), 417–427.
- (5) Dhule, S. S.; Penfornis, P.; Frazier, T.; Walker, R.; Feldman, J.; Tan, G.; He, J. B.; Alb, A.; John, V.; Pochampally, R. Curcumin-Loaded Gamma-Cyclodextrin Liposomal Nanoparticles as Delivery Vehicles for Osteosarcoma. *Nanomedicine* **2012**, *8* (4), 440–451.
- (6) Yoshina-Ishii, C.; Chan, Y. H. M.; Johnson, J. M.; Kung, L. A.; Lenz, P.; Boxer, S. G. Diffusive Dynamics of Vesicles Tethered to a

Fluid Supported Bilayer by Single-Particle Tracking. *Langmuir* **2006**, *22* (13), 5682–5689.

(7) Ferguson, C. G.; James, R. D.; Bigman, C. S.; Shepard, D. A.; Abdiche, Y.; Katsamba, P. S.; Myszk, D. G.; Prestwich, G. D. Phosphoinositide-Containing Polymerized Liposomes: Stable Membrane-Mimetic Vesicles for Protein-Lipid Binding Analysis. *Bioconjugate Chem.* **2005**, *16* (6), 1475–1483.

(8) Ricchelli, F.; Jori, G.; Gobbo, S.; Tronchin, M. Liposomes as Models to Study the Distribution of Porphyrins in Cell-Membranes. *Biochim. Biophys. Acta, Biomembr.* **1991**, *1065* (1), 42–48.

(9) Elani, Y.; Law, R. V.; Ces, O. Vesicle-Based Artificial Cells as Chemical Microreactors with Spatially Segregated Reaction Pathways. *Nat. Commun.* **2014**, *5* (1), 5305.

(10) Kamiya, K.; Takeuchi, S. Giant Liposome Formation toward the Synthesis of Well-Defined Artificial Cells. *J. Mater. Chem. B* **2017**, *5* (30), 5911–5923.

(11) Salehi-Reyhani, A.; Ces, O.; Elani, Y. Artificial Cell Mimics as Simplified Models for the Study of Cell Biology. *Exp. Biol. Med.* **2017**, *242* (13), 1309–1317.

(12) Lee, S. M.; O'Halloran, T. V.; Nguyen, S. T. Polymer-Caged Nanobots for Synergistic Cisplatin-Doxorubicin Combination Chemotherapy. *J. Am. Chem. Soc.* **2010**, *132* (48), 17130–17138.

(13) Al-Jamal, W. T.; Kostarelos, K. Construction of Nanoscale Multicompartment Liposomes for Combinatory Drug Delivery. *Int. J. Pharm.* **2007**, *331* (2), 182–185.

(14) Bolinger, P. Y.; Stamou, D.; Vogel, H. Integrated Nanoreactor Systems: Triggering the Release and Mixing of Compounds inside Single Vesicles. *J. Am. Chem. Soc.* **2004**, *126* (28), 8594–8595.

(15) Renggli, K.; Baumann, P.; Langowska, K.; Onaca, O.; Bruns, N.; Meier, W. Selective and Responsive Nanoreactors. *Adv. Funct. Mater.* **2011**, *21* (7), 1241–1259.

(16) Kisak, E. T.; Coldren, B.; Evans, C. A.; Boyer, C.; Zasadzinski, J. A. The Vesosome - a Multicompartment Drug Delivery Vehicle. *Curr. Med. Chem.* **2004**, *11* (2), 199–219.

(17) Walker, S. A.; Kennedy, M. T.; Zasadzinski, J. A. Encapsulation of Bilayer Vesicles by Self-Assembly. *Nature* **1997**, *387* (6628), 61–64.

(18) Kisak, E. T.; Coldren, B.; Zasadzinski, J. A. Nanocompartments Enclosing Vesicles, Colloids, and Macromolecules Via Interdigitated Lipid Bilayers. *Langmuir* **2002**, *18* (1), 284–288.

(19) Bordi, F.; Cametti, C.; Sennato, S.; Diociaiuti, M. Direct Evidence of Multicompartment Aggregates in Polyelectrolyte-Charged Liposome Complexes. *Biophys. J.* **2006**, *91* (4), 1513–1520.

(20) Marguet, M.; Edembe, L.; Lecommandoux, S. Polymersomes in Polymersomes: Multiple Loading and Permeability Control. *Angew. Chem., Int. Ed.* **2012**, *51* (5), 1173–1176.

(21) Ejima, H.; Richardson, J. J.; Liang, K.; Best, J. P.; van Koeveden, M. P.; Such, G. K.; Cui, J. W.; Caruso, F. One-Step Assembly of Coordination Complexes for Versatile Film and Particle Engineering. *Science* **2013**, *341* (6142), 154–157.

(22) Lee, J.; Cho, H.; Choi, J.; Kim, D.; Hong, D.; Park, J. H.; Yang, S. H.; Choi, I. S. Chemical Sporulation and Germination: Cytoprotective Nanocoating of Individual Mammalian Cells with a Degradable Tannic Acid-Fe-III Complex. *Nanoscale* **2015**, *7* (45), 18918–18922.

(23) Li, W.; Bing, W.; Huang, S.; Ren, J. S.; Qu, X. G. Mussel Byssus-Like Reversible Metal-Chelated Supramolecular Complex Used for Dynamic Cellular Surface Engineering and Imaging. *Adv. Funct. Mater.* **2015**, *25* (24), 3775–3784.

(24) Park, J. H.; Kim, K.; Lee, J.; Choi, J. Y.; Hong, D.; Yang, S. H.; Caruso, F.; Lee, Y.; Choi, I. S. A Cytoprotective and Degradable Metal-Polyphenol Nanoshell for Single-Cell Encapsulation. *Angew. Chem., Int. Ed.* **2014**, *53* (46), 12420–12425.

(25) Kumar, S.; Michael, I. J.; Park, J.; Granick, S.; Cho, Y. K. Cloaked Exosomes: Biocompatible, Durable, and Degradable Encapsulation. *Small* **2018**, *14* (34), 1802052.

(26) Saiz-Poseu, J.; Mancebo-Aracil, J.; Nador, F.; Busque, F.; Ruiz-Molina, D. The Chemistry Behind Catechol-Based Adhesion. *Angew. Chem., Int. Ed.* **2019**, *58* (3), 696–714.

- (27) Huh, N. W.; Porter, N. A.; McIntosh, T. J.; Simon, S. A. The Interaction of Polyphenols with Bilayers: Conditions for Increasing Bilayer Adhesion. *Biophys. J.* **1996**, *71* (6), 3261–3277.
- (28) Simon, S. A.; Disalvo, E. A.; Gawrisch, K.; Borovyagin, V.; Toone, E.; Schiffman, S. S.; Needham, D.; McIntosh, T. J. Increased Adhesion between Neutral Lipid Bilayers - Interbilayer Bridges Formed by Tannic-Acid. *Biophys. J.* **1994**, *66* (6), 1943–1958.
- (29) Tarahovsky, Y. S.; Yagolnik, E. A.; Muzafarov, E. N.; Abdrasilov, B. S.; Kim, Y. A. Calcium-Dependent Aggregation and Fusion of Phosphatidylcholine Liposomes Induced by Complexes of Flavonoids with Divalent Iron. *Biochim. Biophys. Acta, Biomembr.* **2012**, *1818* (3), 695–702.
- (30) Tarahovsky, Y. S.; Kim, Y. A.; Yagolnik, E. A.; Muzafarov, E. N. Flavonoid-Membrane Interactions: Involvement of Flavonoid-Metal Complexes in Raft Signaling. *Biochim. Biophys. Acta, Biomembr.* **2014**, *1838* (5), 1235–1246.
- (31) Holder, G. E.; McGary, C. M.; Johnson, E. M.; Zheng, R. B.; John, V. T.; Sugimoto, C.; Kuroda, M. J.; Kim, W. K. Expression of the Mannose Receptor Cd206 in Hiv and Siv Encephalitis: A Phenotypic Switch of Brain Perivascular Macrophages with Virus Infection. *Journal of Neuroimmune Pharmacology* **2014**, *9* (5), 716–726.
- (32) Kline, S. R. Reduction and Analysis of Sans and Usans Data Using Igor Pro. *J. Appl. Crystallogr.* **2006**, *39*, 895–900.
- (33) Ilavsky, J.; Jemian, P. R. Irena: Tool Suite for Modeling and Analysis of Small-Angle Scattering. *J. Appl. Crystallogr.* **2009**, *42*, 347–353.
- (34) Yefimova, S. L.; Tkacheva, T. N.; Kurilchenko, I. Y.; Sorokin, A. V.; Malyukin, Y. V. Spectroscopic Study of Interactions between Dye Molecules in Micelle and Liposome Nanovolumes. *J. Appl. Spectrosc.* **2013**, *79* (6), 914–921.
- (35) Estes, D. J.; Mayer, M. Giant Liposomes in Physiological Buffer Using Electroformation in a Flow Chamber. *Biochim. Biophys. Acta, Biomembr.* **2005**, *1712* (2), 152–160.
- (36) Zhong, Q. Z.; Pan, S. J.; Rahim, M. A.; Yun, G.; Li, J. H.; Ju, Y.; Lin, Z. X.; Han, Y. Y.; Ma, Y. T.; Richardson, J. J.; Caruso, F. Spray Assembly of Metal-Phenolic Networks: Formation, Growth, and Applications. *ACS Appl. Mater. Interfaces* **2018**, *10* (39), 33721–33729.
- (37) Ejima, H.; Richardson, J. J.; Caruso, F. Metal-Phenolic Networks as a Versatile Platform to Engineer Nanomaterials and Biointerfaces. *Nano Today* **2017**, *12*, 136–148.
- (38) Zhang, R. N.; Li, L.; Liu, J. X. Synthesis and Characterization of Ferric Tannate as a Novel Porous Adsorptive-Catalyst for Nitrogen Removal from Wastewater. *RSC Adv.* **2015**, *5* (51), 40785–40791.
- (39) Lee, J. H.; Gustin, J. P.; Chen, T. H.; Payne, G. F.; Raghavan, S. R. Vesicle-Biopolymer Gels: Networks of Surfactant Vesicles Connected by Associating Biopolymers. *Langmuir* **2005**, *21* (1), 26–33.
- (40) Doucet, M. C.; Jae, H.; Alina, G.; Bakker, J.; Bouwman, W.; Butler, P.; Campbell, K.; Gonzales, M.; Heenan, R.; Jackson, A.; Juhas, P.; King, S.; Kienzle, P.; Krzywon, J.; Markvardsen, A.; Nielsen, T.; O'Driscoll, L.; Potrzebowski, W.; Ferraz Leal, R.; Richter, T.; Rozycko, P.; Snow, T.; Washington, A. Sasview Version 4.2.1.
- (41) Guinier, A.; Fournet, G. *Small-Angle Scattering of X-Rays*; John Wiley & Sons: New York, 1955.
- (42) Balgavy, P.; Dubnickova, M.; Kucerka, N.; Kiselev, M. A.; Yaradaikin, S. P.; Uhrkova, D. Bilayer Thickness and Lipid Interface Area in Unilamellar Extruded 1,2-Diacylphosphatidylcholine Liposomes: A Small-Angle Neutron Scattering Study. *Biochim. Biophys. Acta, Biomembr.* **2001**, *1512* (1), 40–52.
- (43) Zhang, Y. H.; Xuan, S. T.; Owoseni, O.; Omarova, M.; Li, X.; Saito, M. E.; He, J. B.; McPherson, G. L.; Raghavan, S. R.; Zhang, D. H.; John, V. T. Amphiphilic Polypeptoids Serve as the Connective Glue to Transform Liposomes into Multilamellar Structures with Closely Spaced Bilayers. *Langmuir* **2017**, *33* (11), 2780–2789.
- (44) Sanchez-Gaytan, B. L.; Fay, F.; Hak, S.; Alaarg, A.; Fayad, Z. A.; Perez-Medina, C.; Mulder, W. J. M.; Zhao, Y. Real-Time Monitoring of Nanoparticle Formation by Fret Imaging. *Angew. Chem., Int. Ed.* **2017**, *56* (11), 2923–2926.
- (45) Zhang, X. M.; Lin, Y. X.; Gillies, R. J. Tumor Ph and Its Measurement. *J. Nucl. Med.* **2010**, *51* (8), 1167–1170.
- (46) Arora, J. S.; Murad, H. Y.; Ashe, S.; Halliburton, G.; Yu, H.; He, J. B.; John, V. T.; Khismatullin, D. B. Ablative Focused Ultrasound Synergistically Enhances Thermally Triggered Chemotherapy for Prostate Cancer in Vitro. *Mol. Pharmaceutics* **2016**, *13* (9), 3080–3090.